

**O.M. Lavrynenko<sup>1</sup>, M.M. Zahornyi<sup>1</sup>, O.Yu. Pavlenko<sup>1</sup>, E. Paineau<sup>2</sup>**

## **PHOTOCATALYTIC DISCOLORATION OF ORGANIC DYES IN WATER DISPERSION MEDIUM BY ANATASE-BASED BINARY NANOCOMPOSITES**

<sup>1</sup> *I. Frantsevich Institute for Problems of Materials Science of National Academy of Sciences of Ukraine*

*3 Omelianova Pritsaka Str., Kyiv, 03142, Ukraine, E-mail: alena.lavrynenko@gmail.com, m.zahornyi@ipms.kyiv.ua*

<sup>2</sup> *Laboratoire de Physique des Solides, CNRS, Universite Paris-Saclay*

*F-91405 Orsay, France, E-mail: nicolas.paineau@universite-paris-saclay.fr*

Currently, textile and food industries produce a significant volume of effluents containing azo dyes and other organic pollutants. These effluents are serious environmental threats, so new methods for their treatment and the degradation of azo dyes are attracting much attention. Composite materials based on  $TiO_2$  modified by noble metals and nanoceria show high activity in the photodegradation of organic contaminants and are proposed for hydrogen synthesis as well. To optimize the treatment of contaminants, different processes can combine including the strategies of adsorption, photoluminescence, photocatalysis, etc. The synthesized  $TiO_2$ -based nanomaterials (sols, powders) will be exploited for bioremediation due to their small size and surface plasmon resonance from noble metals. Binary nanocomposites based on  $TiO_2$  were obtained by the chemical co-precipitation method from solutions of titanium tetraisopropoxide (TTIP) and inorganic salts of cerium, silver, and palladium. It has been stated that  $TiO_2$  is represented by anatase with primary particle size (CSR) from 8.5 to 16.8 nm, depending on the nature and concentration of the dopant. It is shown that Ag is reduced on the surface of anatase particles and blocks their growth, while Pd and Ce penetrate the titanium dioxide matrix in the form of small clusters with the deformation of the anatase crystal lattice. Nanocomposite particles formed loose and fragile aggregates, which spontaneously dispersed in solutions of dyes with the formation of colloid-stable sols, required the use of a centrifugal field for their sedimentation. Nanoparticles of  $TiO_2$ &Pd were electronegative and others were electropositive according to the values 4.1÷9.6 of ZPC (zero point of charge). It was shown that the particles of all composites sorbed Methylene Blue (MB) without photocatalytic activity under the visible light to any dye. Moreover, anionic dyes such as Orange-G (Or-G) and Methyl Orange (MO) were excellently discolored in the presence of  $TiO_2$ &Pd system; cationic dyes of MB and Rhodamine B (RhB) discolored too with the  $TiO_2$ ,  $TiO_2$ & $CeO_2$ , and  $TiO_2$ &Ag systems under UV light action. As such, photocatalysis tests showed that Orange-G's and MO's discoloration was higher for  $TiO_2$ &Pd (2 wt. %) and  $TiO_2$  systems with the correlation coefficient  $R^2$  0.999.

**Keywords:**  $TiO_2$ -based binary nanocomposites, anatase,  $TiO_2$ &Ag,  $TiO_2$ &Pd,  $TiO_2$ & $CeO_2$ , photocatalysis, UV, discoloration of anionic and cationic dyes, Methyl Orange, Orange-G, Methylene Blue, Rhodamine B

### **INTRODUCTION**

Nowadays, the economical and effective photocatalytic method involves the mineralization of dye molecules over the surface of oxide semiconductor nanomaterial in the presence of light illumination. As such, titanium oxide catalysts have found their wide distribution due to a number of advantages, in particular, low cost, photo-corrosion resistance in a dispersion medium and low toxicity, convenient physical and optical properties, and catalytic efficiency [1]. It is well known that the application of  $TiO_2$  structures in catalysis is limited due to the wide band gap of the semiconductor (~3.2 eV), which prevents the absorption of visible light and the rapid recombination of photogenerated holes ( $h^+$ ) and

electrons ( $e^-$ ) on crystal lattice defects with intensive photoluminescence, and leads to relatively low quantum efficiency. Therefore, the carrying out of catalytic reactions using titanium dioxides requires the influence of UV radiation. In addition, the efficiency of photocatalysis reduced due to the recombination of charge carriers, which prevented the direct way of the surface reactions and accompanied by the rapid occurrence of reverse reactions with combining hydrogen and oxygen and the formation of water [2].

Recently, the proposals to increase the photoactivity of  $TiO_2$  nanomaterials and extend their absorption properties to the spectrum of visible light were widely discussed in scientific publications [3–5]. Several strategies increasing the photocatalytic activity of titanium dioxide

include  $\text{TiO}_2$  sensitization, surface modification of  $\text{TiO}_2$  particles by transition metals, non-metals, or anions, creation of composites based on  $\text{TiO}_2$  with carbon nanotubes, graphene, or semiconductors with a low band gap were used [4]. The mix of titanium dioxide powders corresponding to various crystallographic modifications has been recognized as effective too [5]. One of the considered strategies for improving the activity of  $\text{TiO}_2$  is modification of the nanoparticles (titania) with noble metals [6] or rare earth elements [7]. Noble metals such as Pd, Pt, Au, or Ag, localized on the surface of  $\text{TiO}_2$  particles or introduced into the  $\text{TiO}_2$  matrix as nanoparticles or nanoclusters, exhibit a high Schottky barrier value and thus act as electron traps. Hence, it enhances the photogenerated separation of electron-hole pairs and electron transfer in interphase processes [8].

Silver has become widespread among the noble metals used for  $\text{TiO}_2$  modification [9]. It was stated that the movement of electrons between the conduction band of titanium dioxide and Ag nanoparticles in the structure of the composite was more intense due to the Fermi level of metallic silver compared to titanium dioxide [10]. In addition, silver clusters localized on the surface of titanium dioxide particles were capable to cause the effect of Surface Plasmon Resonance (SPR) at a wavelength of 320÷450 nm near the band gap energy of titanium dioxide (~3.2 eV, 388 nm) [11]. Another noble metal that contributes to the expansion of the efficiency of titanium oxide catalysts to the visible light spectrum is palladium [12]. The Pd ions can improve photocatalytic activity by enhancing the generation of charge carriers, suppressing  $e^-/h^+$  recombination, and increasing the formation of reactive forms responsible for the degradation of organic pollutants [13]. The incorporation of nanoceria into the titanium oxide matrix leads not only to an increase in the catalytic activity of anatase due to  $\text{Ce}^{4+}$  dopants acting as an electron trap in the reaction but electrons captured in the  $\text{Ce}^{4+}/\text{Ce}^{3+}$  centers are transferred on the adsorbed oxygen. Thus, the recombination rate of photoinduced electron-hole pairs decreased, which led to an increase in the photocatalytic activity of  $\text{TiO}_2$  composites doped with  $\text{CeO}_2$  [14]. In general, it has been shown that doping of anatase particles by rare earth elements increased the stability of the structure, reduced the particle size, and improved the catalytic activity of  $\text{TiO}_2$ .

The contact of the particle's surface with the dye molecules influenced the interparticle interaction and accompanied by the processes of sorption, coagulation, and flocculation [15, 16]. The factors affecting the photocatalytic destruction of organic substances are listed as the pH value of the dispersion medium, temperature, concentration of the solution, red-ox conditions in the system, the presence of inorganic anions in the dispersion, etc. [17–19]. At the same time, the pH value of the pollutant can play a key role in dye degradation due to its influence on the sign and magnitude of the surface charge of the catalyst. Therefore, there is a direct correlation between electrokinetic and photocatalysis [20]. The effect of the pH (4÷10) solution on the dye degradation process in acidic and alkaline medium has been shown; for example, the neutralization of Morant Orange-1 molecules in the presence of doped  $\text{TiO}_2$  films [21]. It was found that the efficiency of photocatalysis depended on ZPC of nanoparticles and dye's nature [6, 22–23].

We note that the anionic azo dyes Methyl Orange (acid orange 52) and Orange-G (acid orange 10), as well as cationic dyes - Malachite Green (triarylmethane, basic green), Methylene Blue (triazine, primary blue 9), and Rhodamine B (rhodamine, primary violet 10) are used as model of pollutant for creation new effective catalysts [4, 5, 25, 30–32].

The influence of nature precursor (TTIP and metatitanic acid) applied in the synthesis procedure on the morphology, CSR, and structure characteristics of titanium dioxide nanoparticles was studied in our previous work [24]. The effect of synthesis methods on the phase, chemical composition, and structure of the binary and ternary nanocomposites based on  $\text{TiO}_2$  and their photocatalytic effectiveness on the Malachite Green solution under UV and visible light conditions was studied [25].

The purpose of the work was to study the effectiveness of the cationic and anionic dyes' photocatalytic discoloration by the charged titanium dioxide-based binary nanocomposites in a neutral medium under the visible and UV light action.

## OBJECTS AND METHODS OF THE RESEARCH

Synthesis of the  $\text{TiO}_2$ -based binary nanocomposite particles was performed by the

chemical co-precipitation method using titanium tetraisopropoxide (Acros Organics, NJ, USA) water-ethanol solutions as a matrix material. Cerium nitrate (Sigma-Aldrich, Shanghai, China), argentum nitrate (Sigma-Aldrich, Shanghai, China), and palladium chloride (Sigma-Aldrich, Shanghai, China) were chosen as the doping components. Synthesis was performed in the low alkaline medium in the presence of nucleating and reducing agents [25]. The concentration of the doping species was set at 2 and 4 wt. %. As prepared hydroxide precipitates were washed several times with the water-ethanol solution, filtered, and lyophilized at  $T = 105\text{ }^{\circ}\text{C}$ ; afterward, the dried precipitates were calcined at  $T = 600\text{ }^{\circ}\text{C}$  within 2 h.

The phase composition of the samples was studied by the powder X-ray diffraction phase analysis. XRD data were measured using a powder X-ray diffractometer (DRON 3M) equipped with Cu anode tubes. The scanning step was 0.05–0.1 degrees, exposure – 4 s, range of  $2\Theta$  angles was taken from 15 to  $90^{\circ}$ . Samples were taken at standard temperature. Identification of the phase composition was performed with the help of the International Powder Standards Committee database (JSPDS International Centre for Diffraction Data 1999). Primary particle size (CSR) and crystal lattice parameters of nanocomposites were calculated according to standard methods with the help of the Winscanner 4.0 program, the Lattice program, Debye–Scherrer formula. The morphology of the composite nanostructures was studied by scanning electron microscopy (SEM) using Mira 3 Tescan (Czech Republic) equipped with an energy-dispersive spectrometer (EDS) module Oxford INCA x-act) that determined the chemical composition of the samples.

The zero point of charge (ZPC) of the particles was measured by potentiometric titration of their suspensions (1 wt. % of the disperse phase) where the concentration of NaCl dispersion medium was equal 0.1, 0.01, and 0.001 Mol per  $\text{dm}^3$  using 0.1 M solutions HCl and NaOH. The point in the graph where experimental curves were crossed and showed the ZPC value.

The photocatalytic activity of the composite nanoparticles was tested using MB, RhB, Or-G, and MO water solutions. In all cases, the concentration of the dye was 20 mg/ $\text{dm}^3$ .

The prepared sample of nanopowder (100 mg) was placed in a glass with an addition of 80 mL of the dye water aqueous. The mixture was stirred in the dark for 40 min to reach the adsorption-desorption equilibrium and estimate the sorption activity of the nanocomposites. The duration of the visible light activity test was 30 min, whereas UV activity of the samples was detected in 20, 40, and 60 min supplied by a portable lamp of 300 W Xe 15A. The suspension samples were subjected to centrifugation at 10g for 20 min and removed the nanosized particles from the dispersion medium, acquired colloidal stability under the influence of the dye, and, thus, introduced a significant error in the measurement of light transmission. The optical density was measured by an UV-Vis-NIR Spectrometer at a wavelength from 200 to 800 nm. Mathematical treatment of the measured data allowed us to obtain the kinetic regularities of photocatalysis. Discoloration level was estimated according to maximum peak's intensity MO – 465 nm; RhB – 554 nm; Or-G – 478 nm; MB – 668 nm).

Discoloration degree (%) was calculated via the standard equation:

$$D, \% = (1 - C/C_0) \cdot 100,$$

where  $C_0$  was the initial concentration of the dye solution, and  $C$  was its residual concentration.

## RESULTS AND DISCUSSION

**Physicochemical characteristics of the binary  $\text{TiO}_2$ -based nanocomposites.** X-ray diffraction analysis confirmed the formation of homogeneous nanosized anatase phase for all binary systems based on  $\text{TiO}_2$  with the content of doping impurity of 2 and 4 wt. % (JSPDS No. 21–1272). The XRD pattern of undoped (pure) anatase formed under the same condition was shown for comparison (Fig. 1 a). Other diffractograms (Fig. 2 b–d) corresponded the composite particles containing 4 wt. % of doped components. Moreover, X-ray diffraction measurement did not provide an opportunity to record phases with content in the sample less than 5 %. Thus, it was impossible to register the reflection of noble metals or nanocerium. Since, their small weight percentage (2÷4 wt. %) in the composition of the powder was lower than the sensitivity of the X-ray diffraction method.

At the same time, the calculated crystal lattice parameters of the samples were presented

in Table 1. The values of the elementary cell's parameters and the primary particle's size (CSR) indicated the small variations in the structure of the samples. In particular,  $a$  parameter of the tetragonal anatase crystal lattice varied from 0.3740 nm for the  $\text{TiO}_2\&\text{CeO}_2$  (2 wt. %) system to 0.3775 nm for the pure  $\text{TiO}_2$  powder;  $c$  parameter varied, respectively, from 0.9451 nm for the  $\text{TiO}_2\&\text{Ag}$  system (4 wt. %) to 0.9645 nm for the  $\text{TiO}_2\&\text{CeO}_2$  (4 wt. %) system. The unit cell volumes ranged from 0.133 to 0.134 nm<sup>3</sup> for all studied nanocomposites and did not show the correspondence to the weight part of the admixtures. The CSR of the particles were in the range of 8.3–16.8 nm. So, the biggest value was for  $\text{TiO}_2\&\text{Pd}$  nanocomposites but the smallest value corresponded to  $\text{TiO}_2\&\text{Ag}$  nanocomposites. Hence, we obtained the CSR row of the powders:



The  $d$ -distances (101) of anatase for all composite powders shifted to smaller values compared to the pure  $\text{TiO}_2$  powder (0.35129 nm). However, the expansion of  $\text{TiO}_2$  reflexes compared to the reflexes of the unalloyed sample (Fig. 1 a) indicated the inclusion of cerium and noble metal cations in the anatase structure and did not exclude their replacement of  $\text{Ti}^{4+}$  cations [26].

The degree of tetragonality of the anatase crystal lattice ( $c/a > 1$ ), obtained in the presence of Ag, varied from 2.51 to 2.52, which corresponded to the ratio of the parameters of the standard sample of anatase (JSPDS No. 21–1272) and was equal to 2.51. Taking into account the small values of CSR and  $c/a$ , we can assume the

rapid development of Ag clusters on the anatase surface, which hinders the growth of  $\text{TiO}_2$  particles. It was also shown in [27] that although Ag was not included in the  $\text{TiO}_2$  lattice, and the presence of Ag prevented the growth of anatase grains and promoted the phase transformation of anatase into rutile. Usually, silver was highly dispersed in the composite structure and presented in the metal state. This concept agrees well with the change in powder colour from white to light gray and then to dark gray in our samples.

For the nanocomposites formed in the  $\text{TiO}_2\&\text{Pd}$  and  $\text{TiO}_2\&\text{CeO}_2$  systems, the ratio  $c/a$  increased to 2.56 and 2.57, which indicated the inclusion of cerium and palladium cations in the anatase structure. In particular, the authors [28] showed that small clusters of metallic cerium were well dispersed in the  $\text{TiO}_2$  matrix of the  $\text{TiO}_2\&\text{CeO}_2$  (3 %) system. However, studies of the structure of  $\text{TiO}_2$  catalysts doped with noble metals showed that the diffusion of Pd inside the porous structure of  $\text{TiO}_2$  was quite poor. A relatively large proportion of Pd (< 1 %) used for preparation remains on the outer surface of  $\text{TiO}_2$  [6]. The colour of pure titanium dioxide powders formed in our systems was white, while  $\text{TiO}_2\&\text{Pd}$  powders became light brown colour and  $\text{TiO}_2\&\text{CeO}_2$  powders were characterized by a yellow colour, the intensity of which increased with increasing cerium and palladium content in the composition of the powders. The cationic radii of titanium and noble metals [25] were the following:  $\text{Ti}^{4+}$  (0.042 nm) <  $\text{Pd}^{4+}$  (0.061 nm) <  $\text{Ti}^{3+}$  (0.067 nm) <  $\text{Ce}^{4+}$  (0.087 nm) <  $\text{Ce}^{3+}$  (0.101 nm) <  $\text{Ag}^+$  (0.115 nm).

**Table 1.** Crystal lattice parameters of the binary  $\text{TiO}_2$ -based nanocomposites according to XRD data

System	Crystal lattice parameters					
	$a$ , nm	$c$ , nm	$c/a$	$V$ , nm <sup>3</sup>	CSR, nm	$d_{(101)}$ , nm
$\text{TiO}_2$	0.3775	0.9479	2.51	0.135	12.7	0.35129
$\text{TiO}_2\&\text{Ag}$ (2 wt. %)	0.3774	0.9473	2.51	0.135	8.6	0.35060
$\text{TiO}_2\&\text{Ag}$ (4 wt. %)	0.3761	0.9451	2.51	0.134	8.3	0.34968
$\text{TiO}_2\&\text{Pd}$ (2 wt. %)	0.3746	0.9609	2.56	0.135	14.2	0.35032
$\text{TiO}_2\&\text{Pd}$ (4 wt. %)	0.3767	0.9507	2.53	0.135	16.8	0.34899
$\text{TiO}_2\&\text{CeO}_2$ (2 wt. %)	0.3740	0.9573	2.56	0.134	10.6	0.34832
$\text{TiO}_2\&\text{CeO}_2$ (4 wt. %)	0.3746	0.9645	2.57	0.135	8.5	0.34916

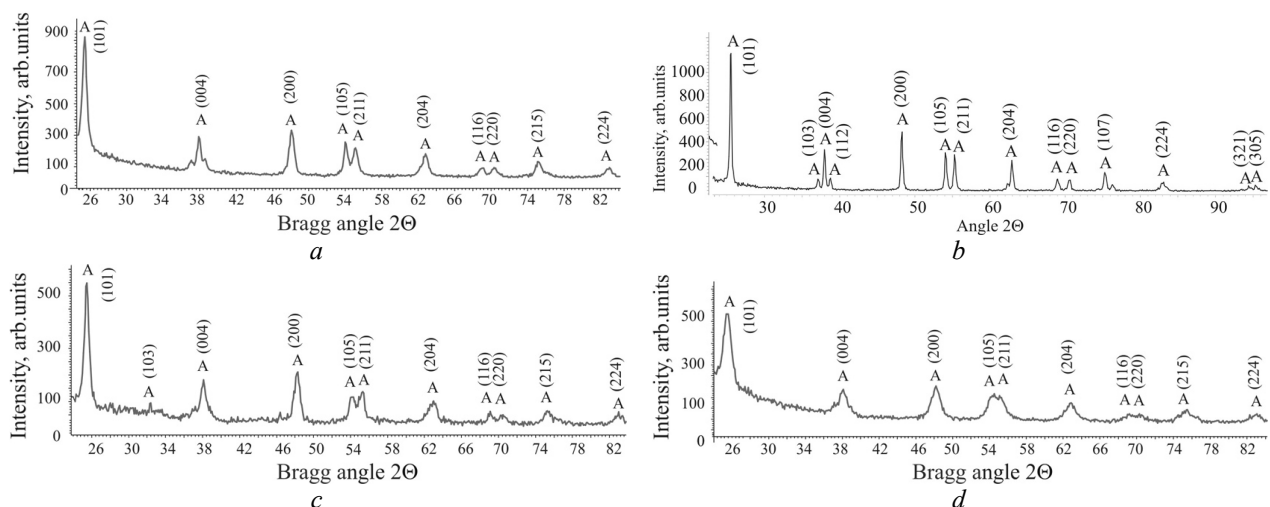


**Fig. 1.** XRD patterns of nanoparticles obtained at  $T = 600\text{ }^{\circ}\text{C}$ : *a* – pure  $\text{TiO}_2$ ; *b* –  $\text{TiO}_2\&\text{Pd}$  (4 wt. %); *c* –  $\text{TiO}_2\&\text{Ag}$  (4 wt. %); *d* –  $\text{TiO}_2\&\text{CeO}_2$  (4 wt. %)

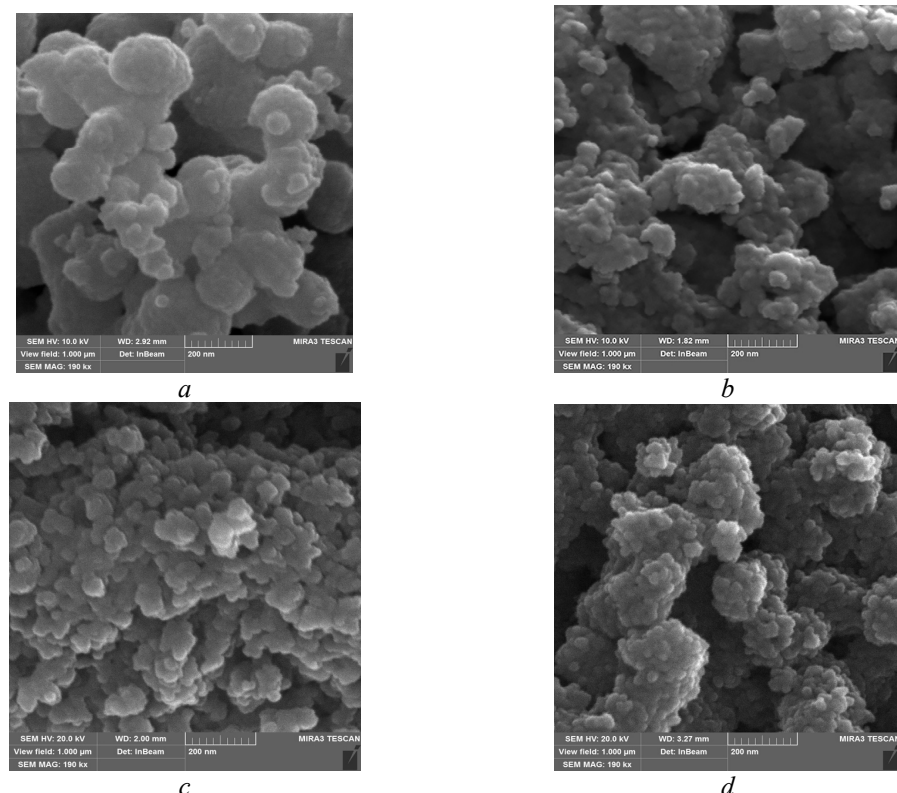


**Fig. 2.** SEM images of nanoparticles formed at  $T = 600\text{ }^{\circ}\text{C}$ : *a* –  $\text{TiO}_2$ ; *b* –  $\text{TiO}_2\&\text{Pd}$  (4 wt. %); *c* –  $\text{TiO}_2\&\text{Ag}$  (4 wt. %); *d* –  $\text{TiO}_2\&\text{CeO}_2$  (4 wt. %)

The morphology of nanocomposite particles obtained in binary systems based on  $\text{TiO}_2$  were performed in Fig. 2. SEM images indicated that nanoscale structures formed loose aggregates (Fig. 2 *a, b, d*); the introduction of Ag into the system increased the degree of crystallization of  $\text{TiO}_2\&\text{Ag}$  particles and the development of

nanocrystal faces (Fig. 2 *c*). The elemental composition of samples according to EDS data indicated the main elements of the composites, such as Ti, O, and Ag, Pd or Ce, and their composition contained minor impurities of auxiliary substances - K, Na, and Cl.

The calculation of tetragonality degree showed that Ag formed small clusters on the surface of anatase particles, but CeO<sub>2</sub> and Pd clusters were included into the structure (matrix) of titanium dioxide or formed very small clusters on the surface that contributed to the color of the powders. The chemical composition of the nanopowders contained small amounts of auxiliary substances in addition to the main (Ti, O) and doping (Ag, Pd, and Ce) elements.

#### *Catalytically active properties of the binary TiO<sub>2</sub> based nanocomposites*

##### *Zero Point of Charge measurement*

The ZPC of dispersed oxides varied from 2 to 10 depending on the synthesis method, the pH value of the medium in which the particles formed, and the composition of auxiliary substances introduced into the system during the synthesis process [23]. For example, the ZPC of anatase formed during the hydrolysis of TTIP varied from 5.9 to 7.2, and for cerium dioxide formed during the hydrolysis of cerium nitrate was 8.8 [23]. An excess of hydroxyl anions raised the pH value at which the particles acquire a zero charge. At the same time, using TiO<sub>2</sub>&Ag composite, the dependence of the potential on pH did not correspond to the average value between the electrokinetic potential dependence of individual TiO<sub>2</sub> and Ag phases and showed a slight horizontal shift towards higher pH values. It was indicated the interaction of individual colloidal particles and the change in the charge of the composite [29].

It was shown that TiO<sub>2</sub>&Ag and TiO<sub>2</sub>&CeO<sub>2</sub> nanoparticles were positively charged, while TiO<sub>2</sub>&Pd particles were negative charged (Table 2). The ZPC of anatase varied between 6.9 and 8.8, depending on the pH of the precipitation of the hydroxide suspension. In general, the ZPC of most nanocomposites were close to neutral but the sign of the particle charge changed in dye solutions due to hydrolysis and deviation of pH values from the pH of the solvent, in our case was water (pH = 6.4).

##### *Sorption activity of nanocomposites in the dark*

The sorption activity of nanocomposite particles was evaluated after 40 min of contact of the dye solution with the nanocomposite. Table 3 showed the discoloration degree of the dye solutions after contact with nanocomposite system. The discoloration degree of Or-G was 13.5 % only for TiO<sub>2</sub>&Pd (4 wt. %); RhB's discoloration degree was 20.0 % only for TiO<sub>2</sub>&CeO<sub>2</sub> (2 wt. %). At the same time, MB was well sorbed by all studied nanocomposites and in terms of intensity of dye extraction formed a series, such as TiO<sub>2</sub>&Pd (11 %) < TiO<sub>2</sub>&Ag (35 %) < TiO<sub>2</sub> (66 %) < TiO<sub>2</sub>& CeO<sub>2</sub> (81 %). This high discoloration degree of MB was due to the morphology nanoparticles and ZPC values of nanostructured TiO<sub>2</sub>&CeO<sub>2</sub>. Besides, electrons captured in the Ce<sup>4+</sup>/Ce<sup>3+</sup> centers were transferred on the adsorbed oxygen of TiO<sub>2</sub> surface.

**Table 2.** Zero point of charge of anatase-based binary nanocomposites formed by the sol-gel method from the TTIP system

Composition of the particles	TiO <sub>2</sub>	TiO <sub>2</sub> &Pd	TiO <sub>2</sub> &Ag	TiO <sub>2</sub> &CeO <sub>2</sub>
Weight % of the dopants	—	2	4	2
ZPC of the particles	6.9–8.8	7.1	4.1	8.4

**Table 3.** Sorption activity of different nanocomposite systems based on TiO<sub>2</sub> in the dark

System	Discoloration degree, %			
	Or-G	RhB	MB	MO
TiO <sub>2</sub>	—	6.0	66.5	10.5
TiO <sub>2</sub> &Ag (2 wt.%)	—	—	35.0	—
TiO <sub>2</sub> &Ag (4 wt.%)	—	4.5	18.0	—
TiO <sub>2</sub> &Pd (2 wt.%)	2.5	0.5	11.0	5.0
TiO <sub>2</sub> &Pd (4 wt.%)	13.5	0.5	4.5	5.0
TiO <sub>2</sub> &CeO <sub>2</sub> (2 wt.%)	—	20.0	74.0	—
TiO <sub>2</sub> & CeO <sub>2</sub> (4 wt.%)	—	4.5	81.0	2.0

*Photocatalytic activity of nanocomposites under Visible light action*

Photocatalysis test of nanocomposite systems was performed under visible light action during 30 min when the systems reached sorption-desorption equilibrium station. The calculation results were presented in Table 4. The obtained data indicated that the nanoparticles of most systems did not show significant activity under the visible light action compared to  $\text{TiO}_2\&\text{CeO}_2$  (2 wt. %) and  $\text{TiO}_2$  systems. Minor increases in the degree of extraction (in the range of 1÷2 %) attributed to

the continuation of the sorption process and were not accounted.

Moreover,  $\text{TiO}_2$  and  $\text{TiO}_2\&\text{Pd}$  composites after contact with MO solutions showed a decrease in the degree of discoloration due to the desorption of dye molecules from the surface of the particles. Besides, increasing dyes colour degree solution was possible due to the conjugated double bonds of the dye molecules with electron-donor or electron-acceptor effects provided by nanocomposite particles presence [31]. The colour of the suspensions was no change, which indicated the absence of processes of dyes decomposition by the catalysis.

**Table 4.** Photocatalytic activity of nanocomposite systems under visible light action

System	Discoloration degree, %		
	Or-G	RhB	MB
$\text{TiO}_2$	—	6.0	51.5
$\text{TiO}_2\&\text{Ag}$ (2 wt. %)	—	—	40.5
$\text{TiO}_2\&\text{Ag}$ (4 wt. %)	—	—	21.0
$\text{TiO}_2\&\text{Pd}$ (2 wt. %)	2.0	5.5	11.0
$\text{TiO}_2\&\text{Pd}$ (4 wt. %)	15.5	1.5	1.5
$\text{TiO}_2\&\text{CeO}_2$ (2 wt. %)	—	55.0	73.5
$\text{TiO}_2\&\text{CeO}_2$ (4 wt. %)	—	3.5	76.0

*Photocatalytic activity of nanocomposites under UV light action*

Photocatalysis test of nanocomposite systems was performed under UV light action during 60 min when the systems reached

sorption-desorption equilibrium station. The calculation results were presented in Table 5. The analysis of the data showed a high photocatalytic discoloration of Or-G, MB, MO dyes for  $\text{TiO}_2\&\text{Pd}$  and  $\text{TiO}_2\&\text{Ag}$  systems:

**Or- G:**  $\text{TiO}_2\&\text{ CeO}_2$  (16.5 %) <  $\text{TiO}_2$  (28.0 %) <  $\text{TiO}_2\&\text{Ag}$  (45.0 %) <  $\text{TiO}_2\&\text{Pd}$  (99.5 %)

**MO:**  $\text{TiO}_2\&\text{CeO}_2$  (6.1 %) <  $\text{TiO}_2\&\text{Ag}$  (27.0 %) <  $\text{TiO}_2$  (63.5 %) <  $\text{TiO}_2\&\text{Pd}$  (93.5 %)

**RhB:**  $\text{TiO}_2\&\text{ CeO}_2$  (36.5 %) <  $\text{TiO}_2$  (69.0 %) <  $\text{TiO}_2\&\text{Ag}$  (73.5 %) <  $\text{TiO}_2\&\text{Pd}$  (81.5 %)

**MB:**  $\text{TiO}_2\&\text{Pd}$  (85.5 %) <  $\text{TiO}_2$  (91.0 %) <  $\text{TiO}_2\&\text{ CeO}_2$  (91.5 %) <  $\text{TiO}_2\&\text{Ag}$  (98.0 %).

It can be seen that the discoloration degree of MB was quite high for all composites and reached 85.5÷98.0 % after 60 min of UV irradiation. However, the best result was obtained for  $\text{TiO}_2\&\text{Ag}$  particles. The effectiveness of the MB discoloration by composites based on  $\text{TiO}_2$  doped with silver was discussed [30]. The neutralization of RhB was 81.5 %. Anionic dye's discoloration degree was 93.5÷99.5 % in the presence of  $\text{TiO}_2\&\text{Pd}$  nanoparticles. In addition, our experiments were carried out with powerful UV lamp (300 W) in the region of 300÷400 nm. UV irradiation energy in the wavelengths range of 300÷400 nm was

typically 500÷300  $\text{kJ}\cdot\text{mol}^{-1}$  [32]. The energy of C-C, C-N, C=C, N=N bonds were 245  $\text{kJ}\cdot\text{mol}^{-1}$ , 203  $\text{kJ}\cdot\text{mol}^{-1}$ , 420  $\text{kJ}\cdot\text{mol}^{-1}$ , and 334.5  $\text{kJ}\cdot\text{mol}^{-1}$ , respectively [33].

The coefficient of correlation  $R^2$  was 0.999 due to the neutralization of Or-G by binary composite  $\text{TiO}_2\&\text{Pd}$  (2 wt. %) and MO discoloration too by  $\text{TiO}_2$  system, which indicated a pseudo-first-order reaction. A similar correlation coefficient was obtained in the extraction of RhB with  $\text{TiO}_2\&\text{Pd}$  (4 wt. %) and MO with  $\text{TiO}_2\&\text{Ag}$  (2 wt. %). In other cases, the coefficient of correlation was 0.93÷0.95, which

maybe indicated a pseudo-second-order reaction of the dyes discoloration.

Therefore, the results of the course of sorption-catalytic processes indicated that the efficiency of the interaction of particles with dye molecules depended on the structure, phase composition, and electrokinetic potential of the particles of binary nanocomposites with ZPC, as

well as the nature of the dyes (acidic or basic), the value of the initial pH of the aqueous solutions of the dyes too. The high discoloration degree of MO, Or-G, and RhB achieved with TiO<sub>2</sub>&Pd (4 wt. %) catalyst and the maximum degree of MB discoloration presented by TiO<sub>2</sub>&Ag (2 wt. %) nanoparticles too.

**Table 5.** The degree of discoloration for dye solutions (%) under UV light during 60 min

System	Discoloration rate, %			
	Or-G	RhB	MB	MO
TiO <sub>2</sub>	28.0	69.0	91.0	63.5
TiO <sub>2</sub> &Ag (2 wt. %)	45.5	73.5	98.0	27.0
TiO <sub>2</sub> &Ag (4 wt. %)	17.5	61.0	87.0	8.5
TiO <sub>2</sub> &Pd (2 wt. %)	62.0	81.5	85.5	37.0
TiO <sub>2</sub> &Pd (4 wt. %)	99.5	76.0	79.5	93.5
TiO <sub>2</sub> &CeO <sub>2</sub> (2 wt. %)	16.5	36.5	91.5	6.5
TiO <sub>2</sub> & CeO <sub>2</sub> (4 wt. %)	14.0	22.0	79.5	—

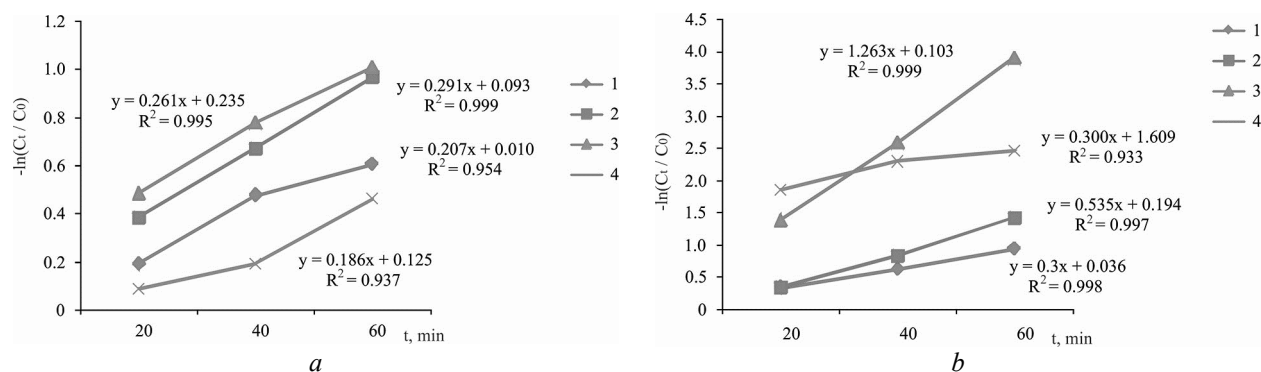


**Fig. 3.** Kinetic of dye's discoloration in the presence of nanoparticles under UV light:  
a – anionic dyes, where numbers correspond to 1 – TiO<sub>2</sub>&Ag 2 wt. % (Or-G); 2 – TiO<sub>2</sub>&Pd 2 wt. % (Or-G); 3 – TiO<sub>2</sub> (MO); 4 – TiO<sub>2</sub>&Pd 4 wt. % (MO); b – cationic dyes, where numbers corresponded to: 1 – TiO<sub>2</sub>&Ag 4 wt. % (RhB); 2 – TiO<sub>2</sub>&Pd 4 wt. % (Rh B); 3 – TiO<sub>2</sub>&Ag 2 wt. % (MB); 4 – TiO<sub>2</sub>&CeO<sub>2</sub> 2 wt. % (MB)

## CONCLUSIONS

The binary nanocomposites based on TiO<sub>2</sub> were obtained by a co-precipitation method from the TTIP and inorganic salts of cerium, silver, and palladium. After heat treatment at  $T = 600^{\circ}\text{C}$ , nanosized powders of anatase doped with the corresponding metals were obtained with their content of 2 and 4 wt. %. The CSR of nanocomposites was  $8.5 \div 16.8 \text{ nm}$ , depending on the nature and concentration of the dopant. The analysis of the structure of the composites showed that silver quickly reduced on the surface of anatase particles and prevents their growth, while palladium and cerium penetrated

into the structure of the TiO<sub>2</sub> matrix in the form of very small clusters because of the deformation of the anatase crystal lattice.

The morphology of nanocomposites presented the particles which formed loose and fragile aggregates that easily destroyed in solutions of dyes and turned into colloidally stable sols, which required the action of a centrifugal field for their precipitation. ZPC measurement showed that TiO<sub>2</sub>&Pd particles were electronegative compared to others. The sorption activity of nanocomposite particles was shown only for MB dye. The activity of nanocomposites was insignificant under the visible light for all dyes. According to the

intensity of the dyes discoloration under the UV radiation with  $R^2$  coefficient correlation activity series was found:

Or-G < MO < RhB < MB for particles  $TiO_2$   
MO < Or-G < RhB < MB for particles  $TiO_2&CeO_2$  and  $TiO_2&Ag$   
RhB < MB < MO < Or-G for particles  $TiO_2&Pd$ .

As such, anionic dyes were excellent discolored by  $TiO_2&Pd$  composite nanoparticles. Thus, synthesized  $TiO_2&Pd$  can

use for hydrogen generation technology synthesis.

#### ACKNOWLEDGEMENTS

The present work was partially supported by the research Pause Program of Laboratoire de Physique des Solides, CNRS, Universite Paris-Saclay, F-91405 Orsay, France.

## Фотокаталітичне знебарвлення органічних барвників бінарними нанокомпозитами на основі анатазу у водному дисперсійному середовищі

О.М. Лавриненко, М.М. Загорний, О.Ю. Павленко, Ерван Панайо

Інститут проблем матеріалознавства ім. І.М. Францевича Національної академії наук України вул. Омеляна Прицака, 3, Київ, 03142, Україна, alena.lavrynenko@gmail.com, m.zahornyi@ipms.kyiv.ua

CNRS, Лабораторія Фізики університету Париз-Сакле  
91405, Орсе, Франція, nicolas.paineau@universite-paris-saclay.fr

Нині текстильна і харчова промисловість виробляє значну кількість стічних вод, що містять азобарвники та інші органічні забруднювачі. Ці стоки становлять серйозну загрозу навколошньому середовищу, тому нові методи їхнього очищення та розклад азобарвників привертають велику увагу. Композиційні матеріали на основі  $TiO_2$ , модифіковані благородними металами та наноцерієм, виявляють високу активність у фотодеградації органічних забруднень, а також пропонуються для синтезу водню. Для оптимізації обробки забруднювачів можна комбінувати різні процеси, включаючи адсорбцію, фотолюмінесценцію, фотокаталіз тощо. Синтезовані наноматеріали на основі  $TiO_2$  (золі, порошки) будуть використовуватися для бioremediaciї через їхній невеликий розмір і поверхневий плазмонний резонанс від благородних металів. Методом хімічного осадження розчинів тетраізопропоксиду титану та неорганічних солей церію, срібла та паладію отримані бінарні нанокомпозити на основі діоксиду титану. Встановлено, що діоксид титану представлений анатазом з ОКР від 8.5 до 16.8 нм в залежності від складу й концентрації допуючої домішки. Показано, що срібло відновлюється на поверхні частинок анатазу та блокує їхній ріст, в той час як паладій і церій розподілені в титан оксидній матриці в формі маленьких кластерів, що призводить до деформації кристалічної структури анатазу. Частинки композитів утворюють пухкі та крихкі агрегати, які самовільно диспергуються у розчинах барвників з утворенням колоїдно-стійких золів, що потребує застосування відцентрованого поля для їхнього осадження. Наночастинки  $TiO_2&Pd$  були електронегативними, а інші – електропозитивними за значеннями 4.1÷9.6 THZ (точки нульового заряду). Показано, що частинки всіх композитів сорбували метиленовий блакитний (МБ) без фотокаталітичної активності у видимому світлі до будь-якого барвника. Крім того, аніонні барвники, такі як Помаранчевий-Ж (П-Ж) і Метил помаранчевий (МП), чудово знебарвлювалися в присутності системи  $TiO_2&Pd$ ; катіонні барвники МБ й родамін В (Род Б) також знебарвлювалися системами  $TiO_2$ ,  $TiO_2&CeO_2$  й  $TiO_2&Ag$  під дією ультрафіолетового світла. Таким чином, фотокаталіз показав, що знебарвлення П-Ж та МП було найвищим для систем  $TiO_2&Pd$  (2 мас. %) та  $TiO_2$  з коефіцієнтом кореляції  $R^2$  0.999.

**Ключові слова:** бінарні нанокомпозити на основі анатазу, анатаз,  $TiO_2&Ag$ ,  $TiO_2&Pd$ ,  $TiO_2&CeO_2$ , фотокаталіз, знебарвлення аніонних і катіонних барвників під впливом УФ, Метиловий Помаранчевий, Помаранчевий Ж, Метиленовий Блакитний, Родамін Б

## REFERENCES

1. Zangeneh H., Zinatizadeh A.A.L., Habibi M. Photocatalytic oxidation of organic dyes and pollutants in wastewater using different modified titanium dioxides: A comparative review. *J. Ind. Eng. Chem.* 2015. **26**: 1.
2. Zeng M. Influence of TiO<sub>2</sub> Surface Properties on Water Pollution Treatment and Photocatalytic Activity. *Bull. Korean Chem. Soc.* 2013. **34**(3): 953.
3. Tahir M., Tasleem S., Tahir B. Recent development in band engineering of binary semiconductor materials for solar driven photocatalytic hydrogen production. *Int. J. Hydrogen Energy.* 2020. **45**(32): 15985.
4. Nur A.S.M., Sultana M., Mondal A., Islam S., Nur F.R., Islam A., Sumi M.S.A. A review on the development of elemental and codoped TiO<sub>2</sub> photocatalysts for enhanced dye degradation under UV-vis irradiation. *J. Water Process Eng.* 2022. **47**:102728.
5. Eddy D.R., Permana M.D., Sakti L.K., Sheha G.A.N., Solihudin, Hidayat S., Takei T., Kumada N., Rahayu I. Heterophase Polymorph of TiO<sub>2</sub> (Anatase, Rutile, Brookite, TiO<sub>2</sub> (B)) for Efficient Photocatalyst: Fabrication and Activity. *Nanomaterials.* 2023. **13**(4): 704.
6. Sescu A.M., Favier L., Lutic D., Soto-Donoso N., Ciobanu G., Harja M. TiO<sub>2</sub> Doped with Noble Metals as an Efficient Solution for the Photodegradation of Hazardous Organic Water Pollutants at Ambient Conditions. *Water.* 2021. **13**(1): 19.
7. Jaramillo-Fierro X., León R. Effect of Doping TiO<sub>2</sub> NPs with Lanthanides (La, Ce and Eu) on the Adsorption and Photodegradation of Cyanide - A Comparative Study. *Nanomaterials.* 2023. **13**(6): 1068.
8. Subramanian V., Wolf E., Kamat P.V. Semiconductor-metal composite nanostructures. To what extent do metal nanoparticles improve the photocatalytic activity of TiO<sub>2</sub> films? *J. Phys. Chem. B.* 2001. **105**(46): 11439.
9. Seery M.K., George R., Floris P., Pilla S.C. Silver doped titanium dioxide nanomaterials for enhanced visible light photocatalysis. *J. Photochem. Photobiol., A.* 2007. **189**(2–3): 258.
10. Selvaraj R., Li X. Enhanced Photocatalytic Activity of TiO<sub>2</sub> by Doping with Ag for Degradation of 2,4,6-Trichlorophenol in Aqueous Suspension. *J. Mol. Catal. A: Chem.* 2006. **243**(1): 60.
11. Torrell M., Adochite R.C., Cunha L., Barradas N.P., Alves E., Beaufort M.F., Rivière J.P., Cavaleiro A., Dosta S., Vaz F. Surface Plasmon Resonance Effect on the Optical Properties of TiO<sub>2</sub> Doped by Noble Metals Nanoparticles. *J. Nano Res.* 2012. **18–19**: 177.
12. Harja M., Sescu A.M., Favier L., Lutic D. Doping Titanium Dioxide with Palladium for Enhancing the Photocatalytic Decontamination and Mineralization of a Refractory Water Pollutant. *Rev. Chim.* 2020. **71**(7): 145.
13. Bai X., Lv L., Zhang X., Hua Z. Synthesis and photocatalytic properties of palladium-loaded three dimensional flower-like anatase TiO<sub>2</sub> with dominant {001} facets. *J. Colloid Interface Sci.* 2016. **467**: 1.
14. Wang J., Meng F., Xie W., Gao Ch., Zha Y., Liu D., Wang P. TiO<sub>2</sub>/CeO<sub>2</sub> composite catalysts: synthesis, characterization and mechanism analysis. *Appl. Phys. A.* 2018. **124**: 645.
15. Yagub M.T., Sen T.K., Afroze S., Ang H.M. Dye and its removal from aqueous solution by adsorption: a review. *Adv. Colloid Interface Sci.* 2014. **209**: 172.
16. Riera-Torres M., Gutiérrez-Bouzán C., Crespi M. Combination of coagulation-flocculation and nanofiltration techniques for dye removal and water reuse in textile effluents. *Desalination.* 2010. **252**(1–3): 53.
17. Akpan U.G., Hameed B.H. Parameters affecting the photocatalytic degradation of dyes using TiO<sub>2</sub>-based photocatalysts: a review. *J. Hazard Mater.* 2009. **170**(2–3): 520.
18. Alejandra I.-S., Valencia A., Nikolay R., Vásquez L., Felipe A. Effect of pH and Themperature on photocatalytic oxidation of methyl orange using black sand as photocatalyst. *Revista Tiempo Económico.* 2017. **1**(1).
19. Pillai I.M.S., Gupta A.K. Effect of inorganic anions and oxidizing agents on electrochemical oxidation of methyl orange, malachite green and 2,4-dinitrophenol. *J. Electroanal. Chem.* 2015. **762**: 66.
20. Leroy P., Tournassat C., Bizi M. Influence of surface conductivity on the apparent zeta potential of TiO<sub>2</sub> nanoparticles. *J. Colloid Interface Sci.* 2011. **356**(2): 442.
21. Vanlalhmingmawia Ch., Lalhriatpuia Ch., Tiwari D., Kim D.-J. Noble Metal Doped TiO<sub>2</sub> Thin Films In The Efficient Removal of Mordant Orange-1: Insights of Degradation Process. *Research Square.* 2021. **29**: 51732.
22. Nazar M.F., Shah S.S., Khosa M.A. Interaction of Azo Dye with Cationic Surfactant Under Different pH Conditions. *J. Surfactants. Deterg.* 2010. **13**: 529.
23. Kosmulski M. The pH-Dependent Surface Charging and the Points of Zero Charge. *J. Colloid Interface Sci.* 2002. **253**: 77.
24. Lavrynenko O.M., Zahornyi M.M., Paineau E., Pavlenko O.Yu., Tyschenko N.I., Bykov O.I. Characteristic of TiO<sub>2</sub>&Ag<sup>0</sup> nanocomposites formed via transformation of metatitanic acid and titanium(IV) isopropoxide. *Materials Today: Proceedings.* 2022. **62**(15): 7664.
25. Lavrynenko O.M., Zahornyi M.M., Paineau E., Pavlenko O.Yu. Synthesis of active binary and ternary TiO<sub>2</sub>-based nanocomposites for efficient dye photodegradation. *Appl. Nanosci.* 2023. **13**: 7365.

26. Gondal M.A., Rashid S.G., Dastageer M.A., Zubair S.M., Ali M.A., Lienhard J.H., McKinley G.H., Varanasi K.K. Sol-Gel Synthesis of Au/Cu-TiO<sub>2</sub> Nanocomposite and Their Morphological and Optical Properties. *IEEE Photonics Journal*. 2013. **5**(3): 2201908.
27. Evcin A., Arlı E., Baz Z., Esen R., Sever E.G. Characterization of Ag-TiO<sub>2</sub> Powders Prepared by Sol-Gel Process. *Acta Phys. Pol. A*. 2017. **132**(3): 608.
28. Zuas O., Hamim N. Synthesis, Characterization and Properties of CeO<sub>2</sub>-doped TiO<sub>2</sub> Composite Nanocrystals. *Mater. Sci.* 2013. **19**(4): 443.
29. Azouri A., Ge M., Xun K., Sattler K., Lichwa J., Ray Ch. Zeta potential studies of titanium dioxide and silver nanoparticle composites in water-based colloidal suspension. In: *Proceedings of Multifunctional Nanocomposites*. 20–22 September 2006, Honolulu, Hawaii.
30. Chen Y.-W., Lee D.-Sh. Photocatalytic Destruction of Methylene Blue on Ag@TiO<sub>2</sub> with Core/Shell Structure. *Open Access Library Journal*. 2014. **1**: 1.
31. Yahodynets P.I., Skrypska O.V., Andriichuk Yu.M. Khimiia barvnykiv: Navchalnyi posibnyk. (Chernivtsi, 2019). [in Ukrainian].
32. Zhygotsky A., Rynda E., Kochkodan V., Zagorniy M., Lobunets T., Kuzhmenko L., Ragulya A. Effect of dispersity and porous structure of TiO<sub>2</sub> nanopowders on photocatalytic destruction of azodyes in aqueous solutions. *J. Chem. Eng.* 2013. **7**: 949.
33. Venkatamaran K. *The Chemistry of Synthetic Dyes*. (Academy Press: London, 1953).

Received 26.09.2023, accepted 19.02.2024